*Bangladesh Journal of Physics*, **19**, 57-66, 2016

# SYNTHESIS AND CHARACTERIZATION OF ZnS NANOPARTICLES PREPARED BY CO-PRECIPITATION METHOD

**M. M. HASAN, M. K. HOSSAIN[1]*, M. M. ALAM[2] AND M. ISLAM[2]**

*Department of ICT, Faculty of Engineering, Comilla University, Comilla, Bangladesh*
*[1]Institute of Electronics, Atomic Energy Research Establishment, Savar, Dhaka 1349, Bangladesh*
*[2]Department AECE, Faculty of Science & Technology, Islamic University, Kushtia, Bangladesh*

*Received on 20.04.2016, Accepted for Publication on 11.06.2016.*

## ABSTRACT

ZnS nanoparticles have been prepared through a simple soft chemical route, namely the chemical co-precipitation method at room temperature. The nanostructures of the prepared capped and uncapped ZnS nanoparticles have been analyzed using X-ray diffraction (XRD) and UV–vis spectrophotometer. The size of the particles is found to be in (6–30) nm range. Optical absorption spectrum of the ZnS nanoparticles exhibits blue shifted relative to that of the bulk ZnS at room temperature due to the quantum confinement effect. It is found that the varying concentration has a tremendous effect on the particle growth. It is observed that particle size decreases with increasing $ZnCl_2$ and capping agent concentration. The particle size of nanoparticles has been calculated from the increased band gap by using the effective mass approximation model, which nearly same as obtained by XRD. A mechanism for the formation of polyvinyl alcohol (PVA) encapsulated ZnS nanoclusters under varying PVA mole ratio has also been suggested.

**Keywords:** ZnS nanoparticles, Chemical synthesis, XRD, Optical absorption, Bandgap.

## 1. INTRODUCTION

The Synthesis and characterization of semiconductor nanoparticles has become an important research area in recent years for size dependent optical properties, because they find great applications in photonic and bio-photonics [1–5].The size dependence of the band gap is the most identified aspect of quantum confinement in semiconductors; the band gap increases as the size of the particles decreases. Among the semiconducting nanomaterials, ZnS is one of the most important semiconducting materials since it can be used in electronic or optoelectronic applications [6] such as in flat-panel displays [7], white light LEDs [8], electroluminescent devices [9], sensors [10], lasers [11], infrared windows [12], ultraviolet (UV) lasers [13], anti-reflection coating on solar cells [14], and solar cells [15]. Zinc sulfide (ZnS), due to its high bulk refractive index (n = 2.36 at 620 nm by Abbe method) and lack of absorption in the visible and near IR region (from 400 nm to 2400 nm), is an attractive material for the use as a suitable inorganic component to improve the optical properties of nanocomposites. Furthermore, ZnS relates to the more popular ZnO in terms of atomic structure and chemical properties. Certain properties of ZnS are unique and advantageous compared to ZnO, that is, ZnS has a larger band gap than ZnO (approximately 3.4 eV [16]), and therefore, it is more suitable for visible-UV light-based devices such as sensors or photo detectors. When the dimensions of nanocrystalline particles approach the exciton Bohr radius, a blue shift occur in the optical absorption spectrum

---

Corresponding Author: E-mail: khalid.baec@yahoo.com

due to the quantum confinement phenomenon.The effective mass model is commonly used tostudy the size dependence of optical properties of quantumdots (QD) system. The advantage of the chemical synthesis is to produce size-controlled, un-agglomerated nanoparticles.

The tunability of the properties of nanoparticles by controlling their size may providean advantage in formulating new composite materialswith optimized properties for various applications.However, applications would be restricted due to different nonradiative relaxations pathways. One of the most important non radiative pathways is surface related defects.To overcome the above-mentioned difficulties, organic and inorganic capping agents are used to passivate the free quantum dots. Many scientific methods have been employed to prepare semiconducting nanoparticles including chemical co-precipitation, chemical vapour deposition, hydrothermal and sol-gel process etc.

In this paper, we report a simple soft chemical method for the synthesis and characterization of ZnS nanoparticles at low temperature by controlling the concentration of the polyvinyl alcohol (PVA) and $ZnCl_2$in order to explore various interesting properties. The size of the prepared ZnS nanoparticles are in the 6–30 nm range as has been confirmed from X-ray diffraction (XRD) peak broadening and absorption spectra. The optical- absorption properties of the prepared nanoparticles are measured. It has found that the blue shift of the absorption edge from their corresponding bulk values due to the quantum confinement effect.

## 2. EXPERIMENTAL

### *2.1 Synthesis of ZnS Nanoparticles*

Uncapped ZnS and PVA capped ZnS nanoparticles have been prepared by a soft chemical approach, namely the chemical co-precipitation method [17] using zinc chloride and sodium sulfide as source materials. All the chemicals used are of AR grade (Merck and SD fine chemicals), used without further purification. Freshly prepared aqueous solutions of the chemicals are used for the synthesis of nanoparticles at room temperature. At first 0.005 M of Zinc chloride ($ZnCl_2$) solution was prepared by dissolving 0.068145 gm of $ZnCl_2$ with 100 ml deionized water and 0.0325 M of $Na_2S \cdot 9\ H_2O$ solution was prepared by 0.15614 gm of $Na_2S \cdot 9H_2O$ with 20 ml deionized water. For the synthesis of ZnS nanoparticles, 0.005M $ZnCl_2$ solution was first vigorously stirred using a magnetic stirrer up to 1.5 h at $70^0$C temperature and then the solution of sodium sulfide is mixed with the solution of Zinc chloride drop wise fashion with the help of an inverted glass bottle-like flasktill the whole solution appears milky. Nitrogen gas is flushed throughout the synthesis using a two-port glass tube in order to avoid oxidation of the particle. Particle growth occurred at this stage. The ZnS nanoparticles most likely form via following solid-state reaction:

$$ZnCl_2(s) + Na_2S \cdot 9H_2O(s) \xrightarrow[\text{Magnetic stirrer}]{70^0\text{C Temperature}} ZnS + 2NaCl + 9H_2O$$

Finally the nanoparticles were collected by centrifugation at 2000 rpm for 15 minutes and washed several times with deionized water and ethanol to remove impuritiesand further purification was made by ultrasonic bath. The precipitates werefinally dried at $110^0$Cfor 4 hours and crushed into fine powder using mortar and pestle. Thus light yellow powder of ZnS nanoparticles were obtained using chemical precipitation technique.For the synthesis of PVA capped ZnS nanoparticles, the desired amount of $ZnCl_2$ and NaS solution was added in drop wise fashion into the PVA solution and dissolved under gentle stirring with presence of nitrogen gas at room temperature. To examine the effect of process parameters on the characteristics of the synthesized nanoparticles, the same experimental procedure was followed by varying the (i) concentration of reactant solution ($ZnCl_2$) and (ii) concentration of PVA.

### 2.2 *Characterization of the Sulphide Nanoparticles*

The ZnS nanoparticles were characterized by X-ray diffraction (XRD) (PHILIPS PW3040 X'pert PRO X-ray diffractometer) [18-19] with $CuK_\alpha$ radiation ($CuK_\alpha$: $\lambda = 1.54178$ Å) and a Nickel filter was used to block $K_\beta$ radiations with $2\theta$ ranging from $25^0$ to $50^0$ at the speed of $2° \text{ min}^{-1}$. Optical Absorbance of the ZnS particles and the PVA were recorded with an UV-Vis spectrophotometer [Model: SHIMADZU (UV-1700pc)] in the range 250–500 nm. Crystallite Size of ZnS nanoparticles were calculated following the Scherrer's equation [20],

$$D = {K\lambda}/{\beta cos\theta} \qquad (1)$$

where K = 0.9, D is the crystallite size of the particle in angstrom or nm, λ is the wavelength of X-ray (CuKα: $\lambda = 1.54178$ Å), β is the full-width at half-maximum (FWHM) after correcting the instrument peak broadening (β expressed in radians), θ is the Bragg's angle or diffraction angle.

## 3. RESULTS AND DISCUSSION

### 3.1 *X-Ray Diffraction Studies*

Fig.1represents the XRD patterns of sample A and sample B (Sample A: 0.001M $ZnCl_2$ and sample B: 0.010M $ZnCl_2$) ZnS nanoparticles. It is to be noted that, in both the figures the peaks observed in the XRD patterns match well with crystalline phase of ZnS [21-23], that indicating the formation of ZnS nanoparticles having hexagonal structure reported in the JCPDS Powder Diffraction File no. 36-1450. Intensities of the four most important peaks of ZnS, namely $28.65^0$, $29.44^0$, $31.90^0$ and $47.35^0$ reflections corresponding to (100), (002), (101) and (110), respectively do not deviate from the powder diffraction file intensities. Broadening of the XRD peaks indicates the formation of ZnS nanocrystals.

Based on the Debye-Scherrer equation, the crystallite size of the nanoparticles were calculated using (002) reflection of the XRD patterns and estimated sizes are 7.2 nm for sample A and 6.8 nm for sample B. However, with the increase of $ZnCl_2$mole ratios, the cluster size decreases. Further, it is to be noted that the effect ofthe temperature is one of the important factors for syntheses method. The peak intensity increases when temperature increases at certain level and therefore decreases particle size [24].

The lattice parameters 'a' and 'c' of the hexagonal structure (planes) are calculated according to the relation [24-29]:

$$\frac{1}{d^2} = \frac{4}{3}\left(\frac{h^2+hk+k^2}{a^2}\right) + \frac{l^2}{c^2} \qquad (2)$$

where d is the inter planar spacing of the atomic planes as determined from the position of the different peaks and the lattice parameters are given in Table 1.

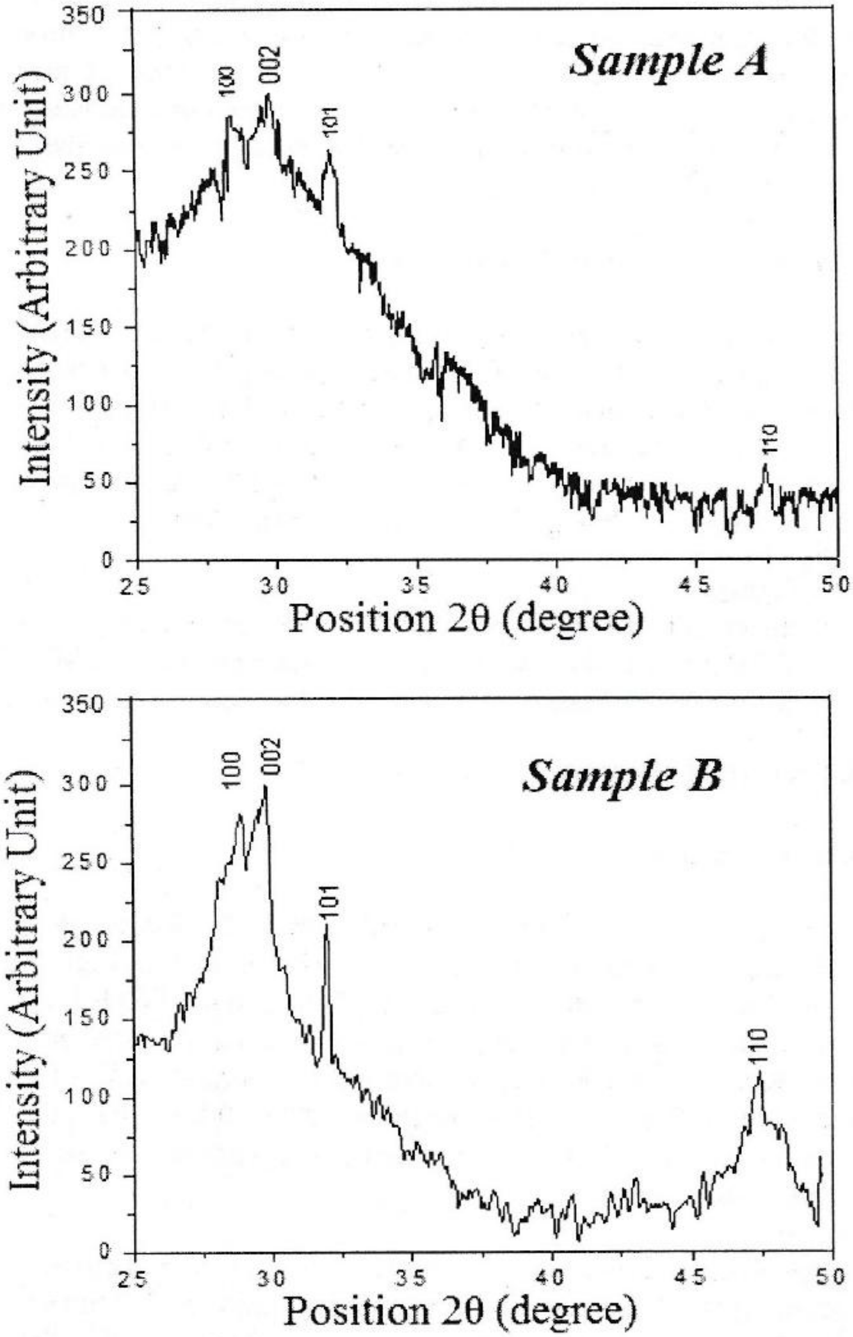

**Fig. 1.** X-ray diffraction patterns of ZnS nanoparticles prepared in various concentrations of zinc chloride. Sample A (0.001M $ZnCl_2$) and sample B (0.010M $ZnCl_2$).

**Table 1.** Lattice parameters of ZnS nanoparticles.

| Sample at (40-45)$^0$C | hkl planes | Lattice parameter | | Average Value | |
|---|---|---|---|---|---|
| | | a (Å) | c (Å) | a (Å) | c (Å) |
| A | (110) & (002) | 3.8326 | 6.0462 | 3.8359 | 6.1067 |
| B | (110) & (002) | 3.8392 | 6.1672 | | |

The lattice parameter values are very close to the standard values but small mismatch to the standard value of c=6.234 Å and a=3.811 Å for the bulk. Such variations in lattice constants with nano-grained materials can be attributed to an increased lattice strain. The strains create local deviation of lattice constants from its bulk value, which is size dependent [30]. As already mentioned the XRD peak broadening could also be due to the strain in addition to the crystallite size of the particles. Hence, the average strain ($\varepsilon$) of the ZnS nanoparticles was calculated using Stokes- Wilson equation [31].

$$\varepsilon_{str} = \frac{\beta}{4\tan\theta} \tag{3}$$

Where $\theta$ is the Bragg angle, $\beta$ is the full width at half maximum of the XRD peak. The dislocation density ($\delta$) was also calculated from the relation [32, 33]:

$$\delta = \frac{15\,\varepsilon_{str}}{aD} \tag{4}$$

where $\varepsilon_{str}$= Lattice strain, a = Lattice parameter and D= Grain size. The average strains and the dislocation densities values are given at Table 2.

From Table 2, it is clear that strain and dislocation density of the two samples A&B decreases as the particle size increases which is a well-known phenomenon [34]. Strain is inherent and natural component of nanograined materials. Due to the large number of grain boundaries and the concomitant short distance between them, the intrinsic strains associated with such interfaces are always present in nanophase films. The dislocations formed in the grain interiors can arrange into dislocation cell boundaries to minimize their strain energy [35]. As a result, sub-grains will form inside the original grains, separated by low angle grain boundary with small misorientations. XRD is able to distinguish these sub-grains with small misorientations [36], even less than 1°–2° and therefore, gives the average size of dislocation cells or sub-grains.

**Table 2.** Structural properties of ZnS (uncapped) nanoparticles.

| Sample | Peak Width ($2\theta$) | Plane (hkl) | Crystallite size (nm) | Lattice strain ($\varepsilon_{str}$) | Dislocation density ($\delta$) lines/$m^2$ | Average Lattice strain ($\varepsilon$) | Average Dislocation density ($\delta_{av}$) lines/ $m^2$ |
|---|---|---|---|---|---|---|---|
| A | 1.13 | (002) | 7.2 | $18.68 \times 10^{-3}$ | $1.01 \times 10^{17}$ | $9.63 \times 10^{-3}$ | $3.66 \times 10^{16}$ |
| | 0.55 | (100) | 14.9 | $9.42 \times 10^{-3}$ | $2.47 \times 10^{16}$ | | |
| | 0.47 | (101) | 17.6 | $7.15 \times 10^{-3}$ | $1.59 \times 10^{16}$ | | |
| | 0.33 | (110) | 26.3 | $3.28 \times 10^{-3}$ | $4.88 \times 10^{15}$ | | |
| B | 1.2 | (002) | 6.8 | $19.92 \times 10^{-3}$ | $1.14 \times 10^{17}$ | $10.4 \times 10^{-3}$ | $4.32 \times 10^{17}$ |
| | 0.70 | (100) | 11.7 | $11.95 \times 10^{-3}$ | $3.99 \times 10^{16}$ | | |
| | 0.55 | (110) | 15.77 | $5.47 \times 10^{-3}$ | $1.36 \times 10^{16}$ | | |
| | 0.27 | (101) | 30.5 | $4.12 \times 10^{-3}$ | $5.28 \times 10^{15}$ | | |

### 3.2 *Optical Absorption Studies (Optical Characterization)*

Fig. 2 shows the absorption spectra of uncapped (Sample A: 0.001M $ZnCl_2$ and sample B: 0.010M $ZnCl_2$) and capped (sample C: 0.00022M PVA and sample D: 0.00033M PVA) nanoparticles. Theabsorption edgesare 307 nm and 297 nm for uncapped ZnS (samples A&B)and 296 nm and 293 nm for capped ZnS (samples B & C) respectively. Band gap energy is calculated using the relation:

$$Eg = h\vartheta = hc/\lambda \tag{5}$$

where h, c, λ, and Eg are the plank's constant, speed of light in vacuum, wavelength and band gap energy of nanoparticles respectively. The blue shift of absorption edge compared to bulk ZnS (onset is at 326 nm) clearly explained by quantum confinement effect of ZnS nanoparticles. From Fig.2, it is clear that the particle size decreases with the increase in molar concentration of $ZnCl_2$and PVA solution. It is well known that the crystallinity and defects of the samples affect the band gap i.e longer wavelength show low crystallinity and defects (Fig.1).

Some theoretical models have been proposed [37, 38], relating the effective band gap of material with the particle size. The simple model predicting the variation of exciton energy with particle size is based on the effective mass approximation (EMA). Here, we calculate the cluster size of ZnS using the following equation [37]:

$$\Delta E = \frac{\hbar^2\pi^2}{2r^2}\left[\frac{1}{m_e^*} + \frac{1}{m_h^*}\right] - \frac{1.786\, e^2}{\varepsilon r} - \frac{0.124\, e^4}{\hbar^2\varepsilon^2}\left[\frac{1}{m_e^*} + \frac{1}{m_h^*}\right]^{-1} \tag{6}$$

Where $m_e^*$ and $m_h^*$ are the effective mass of the electrons and holes respectively, r is the radius of the particles, his Planck's constant and ε is the dielectric constant of the semiconductor. The first term is the kinetic energy of the electrons and holes, the second is their Coulomb attraction and the last term corresponds to the correlation between the two particles. The second and third terms are much smaller than the first term therefore they can be neglected. Thus equation may be expressed as

$$\Delta E = \frac{\hbar^2\pi^2}{2r^2}\left[\frac{1}{m_e^*} + \frac{1}{m_h^*}\right] \tag{7}$$

The value of effective mass of electrons and holes for ZnS are 0.41 $m_e$ and 0.61 $m_e$ [39]. By substituting the band gap values of synthesized samples in equation (7), size of nanoparticles were calculated and are reported in Table 3.

**Table 3.** Particle size and band gap variation with molar concentration.

| Sample | Molar Concentration of $ZnCl_2$ Solution | Molar Concentration of Capping Agent (PVA) | λ (nm) | Energy Band Gap ($E_g$) (eV) | Particle Size (nm) |
|---|---|---|---|---|---|
| A | 0.001 | - | 307 | 4.05 | 4.94 |
| B | 0.010 | - | 297 | 4.18 | 4.00 |
| C | 0.005 | 0.00022 | 296 | 4.20 | 3.92 |
| D | 0.005 | 0.00033 | 293 | 4.24 | 3.74 |

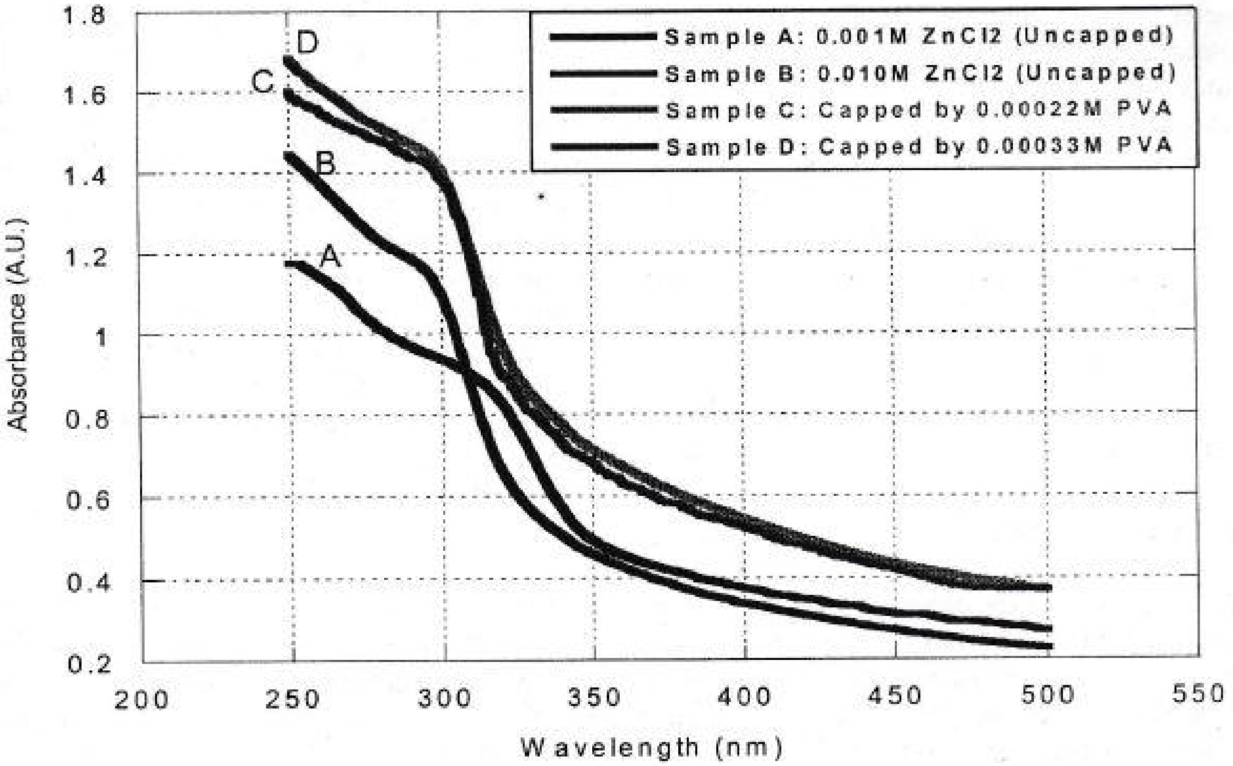

**Fig. 2**. Absorption spectra of uncapped and PVA capped ZnS nanoparticles.

It is clear for samples A and Bthe values of optical band gap '$E_g$' increases with the increase in molar concentration of zinc chloride ($ZnCl_2$) solution and for samples C and Dband gap increases with the increase in molar concentration of capping agent (PVA), therefore decrease particles size. This clearly proves that the necessity of changing molar concentration of $ZnCl_2$ and using capping agent during the synthesis of nanoparticles.

Further, it is to be pointed out in Table 4, the particle size of ZnS nanoparticles estimated from the optical spectraare comparable to those obtained from the XRD analysis, although in some cases minor deviations exist.It is clear that the particle size from XRD and optical spectra is nearly same but it has small difference because of temperature effect on the XRD sample. Nearly same values of particle size from effective band gap and XRD reveal that nanoparticles are spherical in nature [40].This result reveals that molar ratios of $ZnCl_2$ andvarying molar concentration of capping agent (PVA) causes noticeable influence on the size of the ZnS nanoparticles.

**Table 4.** Calculated particle size of ZnS nanoparticles from XRD and absorption peak.

| Sample | Nanoparticle Band gap ($E_{gn}$) eV | Bulk Band Gap ($E_{gb}$) eV | Particle Size from XRD (nm) | Particle Size from optical studies (nm) |
|---|---|---|---|---|
| A | 4.05 | 3.8 | 7.2 | 4.94 |
| B | 4.18 | 3.8 | 6.8 | 4.00 |

Chemical reaction rate directly affects the nucleation and growth process. First, nucleation is faster when the chemical reaction is faster. Second, growth will be strongly influenced by the nuclei number already formed at a given time. A great number of nuclei favours a fast autocatalytic growth, giving rise to a large number of small particles. Chemical reaction controls this kind of growth, being the autocatalytic growth faster as chemical reaction is faster. But in nanoparticle formation, there is another contribution to the growth: molecules on the surface of small particle will tend to diffuse through solution and add to the surface of larger particle (growth by ripening). A slow chemical reaction favors continuous nuclei, keeping always a certain number of nuclei in the system. As a result, growth by ripening can take place during the whole process. This fact explains the bigger particle size obtained from a slow reaction. Rate of reaction depends on the molar concentration of reactants solution and increases with the increase in molar concentration of reactants solution. In the present study, the molar concentration of reactants solution varies from 0.001 M to 0.01 M, the reaction rate is highest for 0.01 M solution and hence the particle size obtained is smallest for 0.01 M solution as compared to other materials in the series, which is in accordance with the above made argument.

## 4. CONCLUSIONS

We conclude that the developed chemical co-precipitation technique has been proved to be highly efficient for the synthesis of ZnSnanoparticles of sizes 6–30 nm that enhanced optical properties within a very short reaction time.This synthesis method being simpler and with cheap chemical components is suitable for industrial large-scale production.Sizes of nanoparticles calculated from Scherrer formula are well matched with sizes calculated from UV-vis spectra.XRD patterns confirm the hexagonal crystalline structure of ZnS and reveals that the strain and dislocation density present in nanophase films. It has been further proved that the zinc chloride mole ratio played an important role in passivating the nanoclusters. Chemical reaction rate affects nucleation and growth process. The nucleation and growth takes place simultaneously, when the chemical reaction is slow. The optical studies show that the absorption peaks of the capped and uncapped ZnS nanoclusters are markedly blue shifted compared to those of the bulk ZnS, which clearly indicate the strong quantum size effect. It is found that the polyvinyl alcohol and zinc chloride concentration has a tremendous effect in the particle growth. Particle sizes were varied with the concentration of zinc chloride and PVA.

## ACKNOWLEDGEMENTS

We would like to thank all concerned with the APECE department, Islamic University for their all-out effort to support us for completing this research. The authors are also thankful to Materials Science Division, Atomic Energy Centre, Dhaka-1000, Bangladesh for extending experimental facilities.

## REFERENCES

[1] A. Henglein, *Chemical Reviews* 89(8), pp 1861 (1989).
[2] M. Nirmal, B. O. Dabbousi, M. G. Bawendi, J. J. Macklin, J. K. Trautman, T. D. Harris and L. E. Brus, *Nature* 383(6603), pp 802 (1996).
[3] M. Bruchez, M. Moronne, P. Gin, S. Weiss and A. P. Alivisatos, *Science* 281(5385), pp 2013 (1998).
[4] W. C. Chan and S. Nie, *Science* 281(5385), pp 2016 (1998).

[5] T. Trindade and P. O. Brien, *Advanced Materials* 8(2), pp 161 (1996).

[6] Z. G. Chen, J. Zou, D. W. Wang, L. C. Yin, G. Liu, Q. Liu and T. Sekiguchi, *Advanced Functional Materials* 19(3), pp 484 (2009).

[7] S. Sahare, S. J. Dhoble, P. Singh and M. Ramrakhiani, *Adv. Mater. Lett* 4(2), pp 169 (2012).

[8] S. Nizamoglu and H. V. Demir, *Journal of Applied Physics* 105(8), pp 083 (2009).

[9] G. O. Müller, R. Mach, B. Selle and H. Ohnishi, *Journal of Crystal Growth* 101(1), pp 999 (1990).

[10] X. Wang, Z. Xie, H. Huang, Z. Liu, D. Chen and G. Shen, *Journal of Materials Chemistry* 22(14), pp 6845 (2012).

[11] I. S. Moskalev, V. V. Fedorov and S. B. Mirov, *Lasers and Applications in Science and Engineering* (USA: International Society for Optics and Photonics), pp 7193 (2009).

[12] Sumitomo Electric Industries, Ltd., *Sei. Tech. Rev.* 71, pp 113 (2010).

[13] C. Onodera, M. Yoshida, T. Shoji and T. Taguchi, *Optical Review* 17(3), pp 159 (2010).

[14] K. H. Kim and J. H. Park, *Transactions on Electrical and Electronic Materials* 5(1), pp 1 (2004).

[15] M. Bredol, K. Matras, A. Szatkowski, J. Sanetra and A. P. Schwab, *Solar Energy Materials and Solar Cells* 93(5), pp 662 (2009).

[16] V. A. Coleman and C. Jagadish, Basic Properties and Applications of ZnO Bulk, *Thin Films and Nanostructures: Processing, Properties, and Applications* (Amsterdam, Netherlands: Elsever Ltd.), pp 1 (2006).

[17] Z. L.Wang, Y. Liu and Z. Zhang, *Handbook of Nanophase and Nanostructured Materials*: (Berlin, Germany: Springer) (2002).

[18] M. K. Hossain, J. Ferdous, M. M. Haque, A. A. Hakim, *World Journal of Nano Science and Engineering* 5(04), pp 107 (2015).

[19] M. K. Hossain, J. Ferdous, M. M. Haque and A. A. Hakim, *Materials Sciences and Applications* 6(12), pp 1089 (2015).

[20] B. D. Cullity, *Elements of X-ray Diffraction*, (USA: Addison–Wesley Company) pp 102 (1978).

[21] J. S. Rita and F. Sasi, *Chalcogenide Letters* 7(4), pp 269 (2010).

[22] J. Li, Q. Zhang, L. An, L. Qin and J. Liu, *Journal of Solid State Chemistry* 181(11), pp 3116 (2008).

[23] Z. Zhao, F. Geng, H. Cong, J. Bai and H. M. Cheng, *Nanotechnology* 17(18), pp 4731. (2006).

[24] L. P. Wang and G. Y. Hong, *Materials Research Bulletin* 35(5), pp 695 (2000).

[25] C. Lan, K. Hong, W. Wang and G. Wang, *Solid State Communications* 125(9), pp 455. (2003).

[26] P. P. Hankare, V. M. Bhuse, K. M. Garadkar, S. D. Delekar and I. S. Mulla, *Semiconductor Science and Technology* 19(1), pp 70 (2004).

[27] K. R. Murali, V. Swaminathan and D. C. Trivedi, *Solar Energy Materials and Solar Cells* 81(1), pp 113 (2004).

[28] J. Y. Choi, K. J. Kim, J. B. Yoo and D. Kim, *Solar Energy* 64(1), pp 41 (1998).

[29] P. O. Brien and J. Mc Aleese, *J. Mater. Chem* 8(11), pp 2309 (1998).

[30] M. Nirmal, D. J. Norris, M. Kuno, M. G. Bawendi, A. L. Efros and M. Rosen, *Physical Review Letters* 75(20), pp 3728 (1995).

[31] R. D. Amaranatha, G. Murali, A. Divya, R. P. Vijayalakshmi and B. K. Reddy, *Journal of Optoelectronics and Advanced Materials* 12(11), pp 2185 (2010).

[32] M. Miyake, K. Murase, T. Hirato and Y. Awakura, Y. *Journal of Electro-Analytical Chemistry* 562(2), pp 247 (2004).
[33] K. Nakamoto, *Infrared Spectra of Inorganic and Coordination Compounds* (New Jersey, USA: John Wiley & Sons) (1970).
[34] A. S. Edelestein and R. C. Camarata, *Nanomaterials: Synthesis, Properties and Applications* (Bristol, UK: Institute of Physics Publishing) pp 170 (1996).
[35] D. A. Hughes and N. Hansen, *Acta Materialia* 48(11), pp 2985 (2000).
[36] T. Ungár, G. Tichy, J. Gubicża and R. J. Hellmig, *Powder Diffraction* 20(04), pp 366 (2005).
[37] Y. Kayanuma, *Physical Review B* 38(14), pp 9797 (1988).
[38] R. Rossetti, J. L. Ellison, J. M. Gibson and L. E. Brus *The Journal of Chemical Physics*, 80(9), pp 4464(1984).
[39] P. E. Lippens and M. Lannoo, *Semiconductor Science and Technology* 6(9A), pp 157. (1991).
[40] R. Tamrakar, M. Ramrakhiani and B. P. Chandra, *Open Nanoscience Journal* 2, pp 12. (2008).